

NANO EXPRESS

Open Access

Adsorption and desorption characteristics of arsenic onto ceria nanoparticles

Qinzhong Feng, Zhiyong Zhang*, Yuhui Ma, Xiao He, Yuliang Zhao and Zhifang Chai

Abstract

The rapid increase in the use of engineered nanoparticles [ENPs] has resulted in an increasing concern over the potential impacts of ENPs on the environmental and human health. ENPs tend to adsorb a large variety of toxic chemicals when they are emitted into the environment, which may enhance the toxicity of ENPs and/or adsorbed chemicals. The study was aimed to investigate the adsorption and desorption behaviors of arsenic on ceria NPs in aqueous solution using batch technique. Results show that the adsorption behavior of arsenic on ceria NPs was strongly dependent on pH and independent of ionic strength, indicating that the electrostatic effect on the adsorption of these elements was relatively not important compared to surface chemical reactions. The adsorption isotherms fitted very well to both the Langmuir and Freundlich models. The thermodynamic parameters (ΔH° , ΔS° , and ΔG°) for the adsorption of arsenic were determined at three different temperatures of 283, 303, and 323 K. The adsorption reaction was endothermic, and the process of adsorption was favored at high temperature. The desorption data showed that desorption hysteresis occurred at the initial concentration studied. High adsorption capacity of arsenic on ceria NPs suggests that the synergistic effects of ceria NPs and arsenic on the environmental systems may exist when they are released into the environment.

Keywords: ceria nanoparticles, arsenic, adsorption, desorption.

Introduction

With the large-scale production and widespread application, the potential environmental risks of engineered nanoparticles [NPs] have consequently attracted much attention since NPs will be unavoidably released to the environment after their production, use, and disposal. To date, the potential environmental effects of NPs, in any quantity, are largely unknown [1-3]; therefore, an understanding of the transport, transfer, and fate of NPs in the environment is an important issue for evaluating their environmental and health impacts.

NPs usually exhibit remarkable physical properties, rapid chemical reactivity, and high sorption capacity for inorganic and organic compounds. Studies of the fate and transport of NPs are largely concerned with how their properties and behavior change over time, whether they will interact with toxic contaminants after being released into the environment or they will change the

anticipated impact of NPs themselves and the toxic contaminants when they interact with one another. For example, recent studies showed that phenanthrene could be adsorbed by iron and copper NPs through hydrophobic effect and dipole interactions between NPs' charged surface and phenanthrene [4]. Carbon nanotubes [CNTs] tend to adsorb toxic chemicals of atrazine, and CNTs with adsorbed atrazine exhibited the toxicities of both the toxic chemicals and CNTs themselves when interacting with living organisms [5]. Therefore, the potential environmental risks of NPs are exerted not only from the NPs themselves, but also from the toxic contaminants adsorbed by them [4,5]. Hence, knowledge of toxic compound adsorption onto NPs is critical and helpful for their risk assessment, and it is also useful for understanding the effect of nanomaterials on the fate of toxic compounds in the environment [4,5]. Unfortunately, to the best of our knowledge, these studies are limited within zerovalent metal NPs, CNTs, and related materials [4,5]; there are no studies that have examined the adsorption and desorption behaviors of toxic contaminants onto metal oxide NPs.

* Correspondence: zhangzhy@ihep.ac.cn

Key Laboratory of Nuclear Analytical Techniques and Key Laboratory for Biomedical Effects of Nanomaterials and Nanosafety, Institute of High Energy Physics, Chinese Academy of Sciences, Beijing, 100049, China

Ceria NPs are considered to be a representative member of an industrially important class of metal oxide NPs [6,7]; they can be used as automotive catalytic converters [8], UV-blocking agents [9], and single, nano-wire-based gas sensors [10]. Indeed, ceria NPs are on the OECD list of priority nanomaterials for immediate testing. However, at present, little ecotoxicity data are available. Previous studies have demonstrated that ceria NPs have toxic effects on cells [11,12], aquatic organisms [13,14], and plants [15]; however, other reports show that ceria NPs are able to rescue HT22 cells from oxidative stress-induced cell death [16] and protect against the progression of cardiac dysfunction [17]. These contradictory results suggest the complex behaviors of ceria NPs in the environment.

Arsenic is one of the most toxic elements and is found virtually in all environmental systems as a result of both geological processes and anthropogenic activities [18,19]; the USEPA has set a maximum contaminant level for arsenic at $10 \mu\text{g L}^{-1}$ in drinking water [20]. Adsorption with metal oxides has been widely used to remove these contaminants because of its effectiveness and simplicity for point-of-use applications. However, since the environmental release of ceria NPs from various applications, the NPs' solid surface interactions with organic contaminants, such as arsenic, have become increasingly important, and the subsequent behavior and effects of the released NPs must be considered an urgent need.

Information on the interaction of free and aggregated NPs with adsorbed chemicals is lacking from the literature, although studies suggest that the adsorption of phenanthrene on nanosized zerovalent iron and copper significantly decreases with the increase in pH, that naphthalene exerted significant competition adsorption with phenanthrene [4], and that Th(IV) adsorption onto oxidized MWCNTs is endothermic [21]. The present work investigated the adsorption and desorption behaviors of arsenic onto ceria NPs. The objectives include (1) to quantify and predict the adsorption behavior of arsenic on ceria NPs under different pH and ionic strength, (2) to determine adsorption isotherms and analyze regressively experimental data with Langmuir and Freundlich models, (3) to study the adsorption of arsenic at different temperatures and measure the adsorption thermodynamic parameters (i.e., ΔH° , ΔS° , ΔG°), and (4) to investigate the desorption behavior of arsenic at the ceria NPs' surface using batch adsorption experiments.

Experimental details

Materials and methods

All chemicals used were of analytical reagent grade. Milli-Q water ($18.2 \text{ M}\Omega \text{ cm}$, Millipore, Beijing, China) was used for all solution preparation. Stock solutions of

arsenic were purchased from the National Institute of Metrology (Beijing, China). These stock solutions were kept at 4°C in darkness. Working solutions of arsenic (0.4 to $40.0 \mu\text{g L}^{-1}$) were prepared daily by dilution of the stock solution with HCl. Working solutions of 20% (*w/v*) potassium tetrahydroborate were prepared daily by dilution of the KBH_4 stock solution in 5% NaOH. Pre-reducing solutions containing 10% (*w/v*) thiourea (Beijing Chemical Works, Beijing, China) and 10% (*w/v*) ascorbic acid (Sigma, Sigma-Aldrich Corporation, St. Louis, MO, USA) were prepared fresh daily in water. Glassware used for the determination of arsenic was soaked in a 10% (*v/v*) nitric acid solution and rinsed with Milli-Q water.

Preparation and characterization of ceria NPs

Ceria NPs used in the experiments were synthesized using a precipitation method as described in our former reports [16,22,23]. The resulting ceria NPs were characterized with a Tecnai G^2 20 S-Twin transmission electron microscope (FEI Company, Tokyo, Japan) operated at 200 keV and with dynamic light scattering, using a Coulter NicompTM 380 ZLS Particle Size Analyzer (Santa Barbara, CA, USA). The surface area was characterized by nitrogen adsorption/desorption analysis of Brunauer-Emmett-Teller (Autosorb-1, Quantachrome Instruments, Boynton Beach, FL, USA).

The X-ray diffraction [XRD] patterns for ceria NPs were recorded on an X'Pert PRO (PANalytical B.V., Almelo, The Netherlands) with monochromatized $\text{Cu K}\alpha$ radiation. The particle size of CeO_2 was calculated from the Scherrer formula using the (220) diffraction peak of the respective cerium oxide [24].

Adsorption experiments

Adsorption isotherms by batch studies were conducted in 7-mL capped centrifuge tubes. Each tube containing 5-mL varying concentrations of arsenic was mechanically shaken on a horizontal motion shaker for 24 h (preliminary experiments had shown that all solid-solution mixtures reached apparent equilibrium within 2 h) at room temperature (25°C). Thermodynamic parameters associated with the adsorption processes were carried out in temperatures of 283, 303, and 323 K. After centrifugation (10,000 rpm for 10 min), the supernatant was sampled and analyzed. The concentration of ceria NPs used for the adsorption experiments was 5 g L^{-1} . Initial concentrations of arsenic were ranged from 0.4 to $40.0 \mu\text{g L}^{-1}$. All experiments were conducted in triplicate.

The solution pH plays a critical role in the adsorption of metalloid ions onto various adsorbents. To optimize the pH for maximum removal efficiency, a sorption experiment was conducted in the initial pH range from 1.0 to 13.0, adjusted using HCl or NaOH.

For ionic strength effect tests, the desired initial sodium nitrate was from 1×10^{-8} to 1.0 mol L^{-1} , arsenic was added, and the batch equilibration was initiated immediately. The effect of H_2SiO_3 colloid and $\text{Fe}(\text{OH})_3$ colloid on As(III) and As(V) adsorptions was examined with the concentration from 2×10^{-6} to 0.1 mmol L^{-1} and from 1×10^{-7} to 0.05 mmol L^{-1} for H_2SiO_3 colloid and $\text{Fe}(\text{OH})_3$ colloid, respectively.

Desorption experiments

Desorption experiments of arsenic were carried out in sequential decant-refill steps immediately following the completion of the sorption experiments. The supernatant (4.0 mL) was removed and immediately replaced by the same volume of background solution (0.01 M NaNO_3), and the vials were resealed and shaken. After 24 h of equilibration, the vials were centrifuged, arsenic in the supernatant was determined, and the amount of arsenic desorbed was calculated from mass differences. The above process was repeated for four complete cycles. All samples were performed at least in triplicate.

Speciation and analysis of arsenic by hydride generation-atomic fluorescence spectrometry

The AFS-9800 atomic fluorescence spectrometer (Beijing Kechuang Haiguang Instrument Co., Ltd, Beijing, China) was used for arsenic determination. The arsine was generated by adding precise, known volumes of the sample, a reducing solution of potassium tetrahydroborate solution (20%) and hydrochloric acid (10%) using an autosampler. Also, a pre-reducing solution (thiourea 10% and ascorbic acid 10%) was used to pre-reduce arsenic(V) to arsenic(III) when the task was to speciate

arsenic(III) and arsenic(V). Arsenic(V) was determined by the difference between total inorganic arsenic and arsenic(III).

Results and discussion

Characterization of ceria NPs

Precipitation method is an attractive, simple, and seemingly general method for producing high-quality ceria NPs under optimum synthesizing conditions. The average particle diameter was $6.6 \pm 0.9 \text{ nm}$ (Figure 1a). BET analysis demonstrated that the ceria NPs had high specific surface areas which were about $86.85 \text{ m}^2 \text{ g}^{-1}$. The size distribution of the hydrodynamic diameter of ceria NPs was about $44.8 \pm 1.6 \text{ nm}$.

The results of XRD in Figure 1b showed that ceria NPs were a single-phase, cubic, calcium fluoride-type structure with space group Fm3m, and no evidence was found for the existence of impurities in the products which was consistent with other reports [25].

Adsorption isotherms

Langmuir and Freundlich isotherms were employed to describe the adsorption of arsenic on ceria NPs at 283, 303, and 323 K. The equation of the Langmuir isotherm is given as Equation 1:

$$\frac{C_e}{q_e} = \frac{1}{q_{\max}K_L} + \frac{C_e}{q_{\max}} \quad (1)$$

The adsorption capacity q_{\max} and adsorption constant K_L can be determined from the slope and intercept of a linearized plot of C_e/q_e against C_e .

The Freundlich isotherm is derived by assuming a heterogeneous surface with a nonuniform distribution of

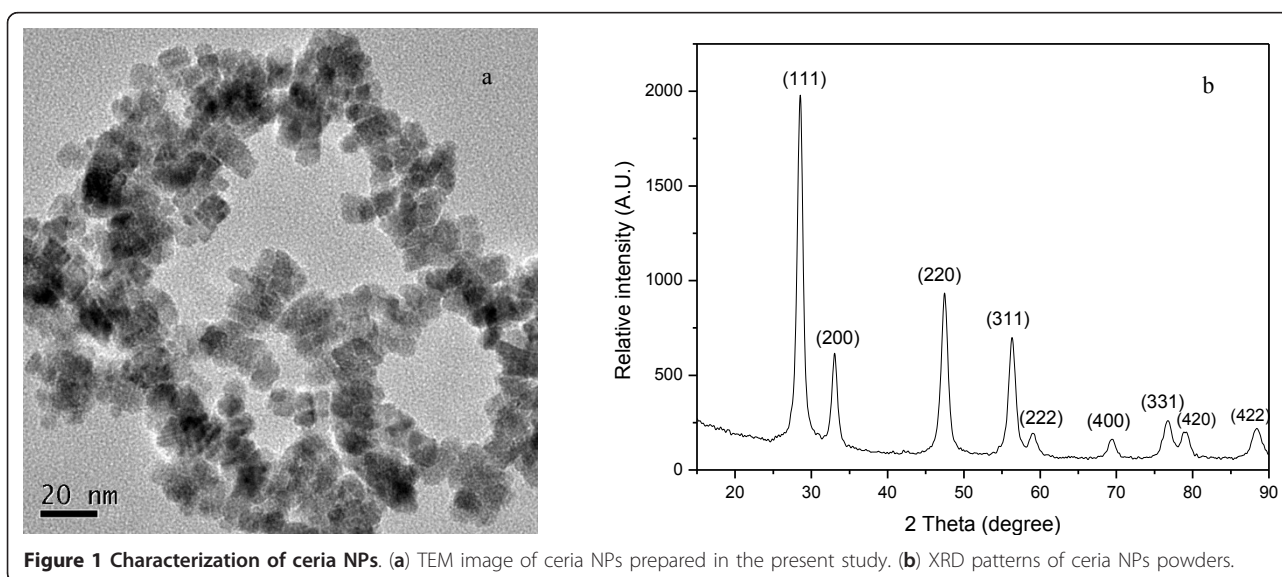


Figure 1 Characterization of ceria NPs. (a) TEM image of ceria NPs prepared in the present study. (b) XRD patterns of ceria NPs powders.

the heat of sorption over the surface. It can be expressed as follows:

$$q_e = K_f C_e^{1/n} \quad (2)$$

The equation can be written as a linearized form:

$$\ln(q_e) = \ln(K_f) + (1/n)\ln(C_e), \quad (3)$$

where K_f and n are the Freundlich constants: n gives an indication of how favorable the adsorption is, and K_f ($\text{mg/g (L/mg)}^{1/n}$) is the adsorption capacity of the adsorbent. If the value of $1/n$ is lower than 1, it indicates a normal Freundlich isotherm; otherwise, it is indicative of cooperative adsorption. The Freundlich constants can be obtained from the plot of $\log q_e$ versus $\log C_e$.

Both Freundlich model and Langmuir model were tested for fitting the arsenic adsorption data. Based on those model equations, the adsorption parameters q_{\max} , K_L , K_f , and n , and the correlation coefficient values (R) of arsenic onto ceria NPs were obtained (Table 1). As seen in Table 1, the adsorption of arsenic onto ceria NPs was well fitted to the Langmuir isotherm model with high R (0.9695 to 0.9815), and this result may be due to the homogeneous distribution of active sites on the surface of ceria NPs. Furthermore, the values of R_L for the Langmuir isotherm were between 0 and 1, and the Freundlich constant $1/n$ was smaller than 1 (0.43 to 0.66), indicating a favorable process. The high adsorption capacity (q_{\max} 17.08 to 18.05 mg g^{-1}) in the present work reveals that the combination of ceria NPs and arsenic may be efficacious on the environment. The adsorption of arsenic (q_{\max} and K_f in the Langmuir model and the Freundlich model, respectively) increased with the rise in temperature, illuminating an endothermic process for arsenic adsorption onto ceria NPs. The adsorption isotherm was higher at 323 K than the other two isotherms, whereas the adsorption isotherm at 283 K was the lowest. The results indicated that the adsorption of arsenic onto ceria NPs was favored at high temperature and was blocked at low temperature.

Table 1 Isotherm model constants of three isotherm models for arsenic adsorption onto ceria NPs

Model	Parameters	Temperature (K)		
		283	303	323
Langmuir model	q_{\max} (mg g^{-1})	17.08	18.02	18.15
	K_L (L mg^{-1})	0.063	0.066	0.24
	R	0.9695	0.9704	0.9815
Freundlich model	K_f (mg g^{-1}) (L mg^{-1}) ^{1/n}	1.32	1.40	2.32
	n	1.54	1.52	1.77
	R	0.9957	0.9948	0.9966

q_{\max} , adsorption capacity; K_L , adsorption constant; K_f and n , Freundlich constants; R , correlation coefficient.

Thermodynamic parameters associated with the adsorption processes

The thermodynamic adsorption parameters can be calculated from the variation of the thermodynamic equilibrium constant K_0 under different temperatures. The standard molar free energy of adsorption [ΔG^0] is calculated from the relationship:

$$\Delta G^0 = -RT \ln K_0. \quad (4)$$

The average standard enthalpy [ΔH^0] is obtained from the slope of the linear variation of $\ln K_0$ versus $1/T$.

$$\ln K_0 = -\frac{\Delta H^0}{RT} + \text{constant}. \quad (5)$$

The standard entropy [ΔS^0] is calculated from:

$$\Delta S^0 = (\Delta H^0 - \Delta G^0)/T. \quad (6)$$

The thermodynamic adsorption parameter values obtained were given in Table 2. The adsorption enthalpy of arsenic onto ceria NPs was 17.89 kJ mol^{-1} , indicating that the adsorption process of arsenic onto ceria NPs was endothermic. It was reported that the enthalpy of physisorption was smaller than 20 kJ mol^{-1} [22]. Based on the above ΔH^0 , it suggests that the adsorption of arsenic onto ceria NPs is a physisorption process. The positive adsorption entropy indicated that the degrees of freedom increased at the solid-liquid interface during the adsorption of arsenic onto ceria NPs. ΔG^0 values were in the range of -1.40 to -4.18 kJ mol^{-1} when the adsorption temperature was from 283 to 323 K, and the negative values of ΔG^0 indicated that the adsorption process was spontaneous. The thermodynamic adsorption data indicated that the adsorption of arsenic onto ceria NPs was an endothermic process, and the process was favorable at high temperature. The results were consistent with the adsorption isotherm results.

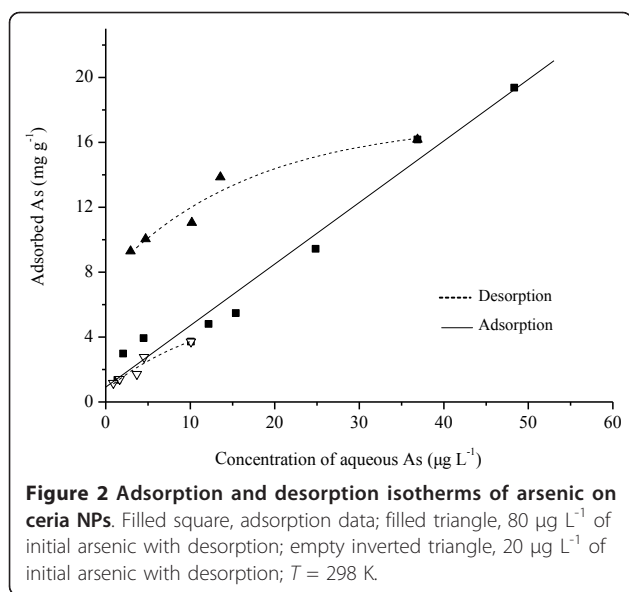
Adsorption and desorption

Figure 2 shows the adsorption and desorption isotherms of arsenic on ceria NPs. There would be a corresponding concentration-dependent effect in this study: the

Table 2 Thermodynamic parameters for arsenic adsorption onto ceria NPs

Temperature (K)	Thermodynamic parameters			
	$\ln(K_0)$	ΔG^0 (kJ mol^{-1})	ΔH^0 (kJ mol^{-1})	ΔS^0 ($\text{J mol}^{-1} \text{K}^{-1}$)
283	0.59	-1.40	17.89	71.52
303	0.65	-1.65	17.89	70.51
323	1.56	-4.18	17.89	80.78

ΔG^0 , standard molar free energy of adsorption; ΔH^0 , average standard enthalpy; ΔS^0 , standard entropy.



desorption of ceria NPs had no significant desorption hysteresis for 20 µg L⁻¹ of arsenic, while it had significant desorption hysteresis when the initial concentration of arsenic was 80 µg L⁻¹ with the thermodynamic index of irreversibility ranging from 0.58 to 0.95.

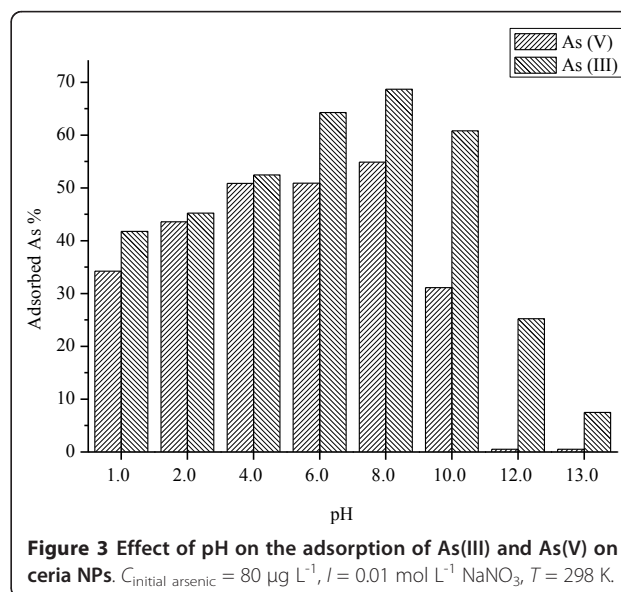
Hysteresis is referred to as irreversible adsorption which is reproducible and originates from a shift in the equilibrium point when a reaction approaches equilibrium from desorption direction rather than sorption [4,26,27]. Similar result was reported by Shirvani et al. that the quantity of Cd desorbed from the minerals after five cycles of desorption was depending on the initial load of Cd on the minerals [26]. Recent studies supported irreversible deformation as the cause of hysteresis in flexible solids, such as natural organic matter and organoclays [5,27]. During the adsorption-desorption cycle, pore deformation may result in some of adsorbent transferred to sites in the solid where free exchange with molecules in the bulk fluid phase is no longer possible.

Desorption of inorganic and organic contaminants from the adsorbent is rapidly gaining recognition owing to its importance to the fate, toxicity, and transport of these contaminants in the environmental system. If the contaminants would be released from the adsorbent in significant concentrations, either in the environmental or biotic mediums, they would be a risk for living organisms. In this work, high adsorption capacity and reversible adsorption of arsenic on ceria NPs suggest that ceria NPs may influence the fate and behavior of arsenic in the environment. Thus, ceria NPs with arsenic may exhibit synergistic effects when interacting with living organisms.

Adsorption characteristics of arsenic(III) and arsenic(V) in different environmental conditions

Inorganic arsenic has four oxidation states: +5, +3, 0, and -3. In the soil/water environment, it is mainly present in the +3 and +5 oxidation states. In reduced environments, arsenious acid is a common arsenic(III) aqueous species, whereas oxidized environments contain more arsenic(V) aqueous species. These two aqueous species may adsorb onto inorganic and organic components and precipitate in a variety of forms. The environmental fate of arsenic in subsurface environments is highly dependent on the arsenic speciation, pH, ionic strength, and the presence of adsorbents such as metal oxides. Furthermore, there are many kinds of colloidal solutions with different charges in water, for example, in general, H₂SiO₃ colloid surface has a negative charge and Fe(OH)₃ colloid surface has a positive charge, which may affect the adsorption of arsenic on ceria NPs. However, little investigation had been conducted on the adsorption of arsenic by ceria NPs in different colloidal solutions. The experiments below were carried out to investigate the adsorption characteristic of arsenic onto ceria NPs in different environmental conditions.

Both arsenate and arsenite adsorptions on ceria NPs as a function of solution pH exhibited a parabolic adsorption curve which was showed in Figure 3. Adsorption increased with increasing solution pH from pH 1 to 6 and then decreased with increasing pH from pH 6 to 13 for arsenate, which was similar to the report that arsenate adsorption on the clays increased with increasing solution pH from pH 3 to 5 and decreased with increasing solution pH from pH 5 to 9 [28]. As for arsenite, adsorption increased with increasing solution pH from pH 1 to 8 (the maximum adsorption was 70%) and then



decreased with increasing pH from pH 8 to 13; a similar behavior was found for arsenite adsorption on the clays and amorphous Al oxide [28]. The maximum adsorption of arsenite occurs in the weak alkaline region, up to pH 10; OH⁻ competition for the arsenite centers at high pH values which leads to the decreasing adsorption.

From Figure 3, it could also be found that arsenite is commonly more strongly adsorbed on ceria NPs than arsenate especially when pH was above 9. Theoretically, arsenate is commonly more strongly adsorbed on ceria NPs than arsenite since arsenate presents as H₂AsO₄⁻ and HAsO₄²⁻ when pH is from 2 to 8, while arsenite presents as As(OH)₃⁰ species. Some reports showed that at all pH values, arsenic(V) was more strongly bound than arsenic(III) [28-30]. Thus, further experiments in our future study should be carried out to study the adsorption mechanism.

The effects of ionic strength on the adsorption of arsenic(III) and arsenic(V) onto the surfaces of ceria NPs were presented in Figure 4. The amount of arsenic(III) and arsenic(V) adsorbed by ceria NPs was stable with increasing ionic strength from 1 × 10⁻⁸ to 1.0 mol L⁻¹ NaNO₃. Therefore, ionic strength generally had very minor or no impact on the adsorption in this study. Similar results were also observed by other reports when iron oxide or other sorbents were used [31-35].

The ionic strength can influence the double-layer thickness and interface potential; thereby, it can affect the binding of the sorbed species [36,37]. The specific and nonspecific adsorptions can be distinguished by evaluating the effect of ionic strength on anion partitioning [37]. It was reported that the specific adsorption is unaffected by the change in ionic strength, whereas

the nonspecific adsorption is likely to be influenced greatly by the change of ionic strength because of the competitive adsorption with counteractions. The insignificant impact of ionic strength indicated that the specific adsorption was found on the adsorption of arsenic(V) and arsenic(III) by ceria NPs which resulted from an inner sphere complex formation between arsenic and the surface of ceria NPs. The strong pH dependence and ionic strength independence further indicate that the adsorption mechanism is mainly surface complexation rather than ion exchange.

H₂SiO₃ colloid was homemade with the particle size of 50 nm. Figure 5 reveals that arsenic adsorption on ceria NPs increased significantly with the increasing of H₂SiO₃ colloid concentration from 2 × 10⁻⁶ to 1 × 10⁻⁵ mmol L⁻¹, while it was stable when H₂SiO₃ colloid concentration was from 2 × 10⁻⁴ to 0.1 mmol L⁻¹. Meanwhile, ceria NPs had lower adsorption capacity for As(III) than for As(V) with the existence of H₂SiO₃ colloidal solution. The possible reason may be the different pH in these solutions. When the concentrations of H₂SiO₃ colloidal solution were lower than 0.001 mol L⁻¹, the pH values were from 5.35 to 5.91. Acid dissociation [pK_a] values for arsenious acid are as follows: pK_a¹ = 9.2 and pK_a² = 12.1, while pK_a values for arsenic acid are pK_a¹ = 2.3, pK_a² = 6.8, and pK_a³ = 11.6. Therefore, at pH 5.35 to 5.91, the surface has a net positive charge; As(III) exists in neutral H₃AsO₃⁰ which has less influence than the adsorption for negatively charged As(V) species which exists in H₂AsO₄⁻. The inflections or maxima in the adsorption of arsenic at pH values close to their pK_a values are a well-documented phenomenon [38,39].

Fe(OH)₃ colloidal solution was synthesized in our laboratory, and TEM showed that Fe(OH)₃ particle was a nanorod with 30 to 70 nm in long diameter. NPs with a high specific surface area tend to adsorb a large variety

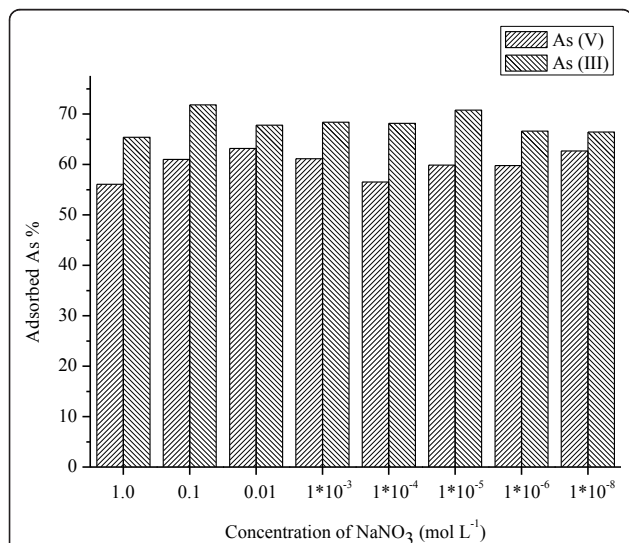


Figure 4 Effect of ion strength on the adsorption of As(III) and As(V) on ceria NPs. C_{initial arsenic} = 80 μg L⁻¹, T = 298 K.

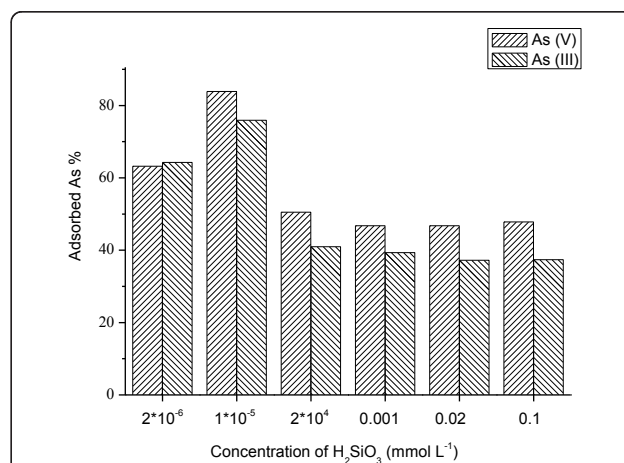
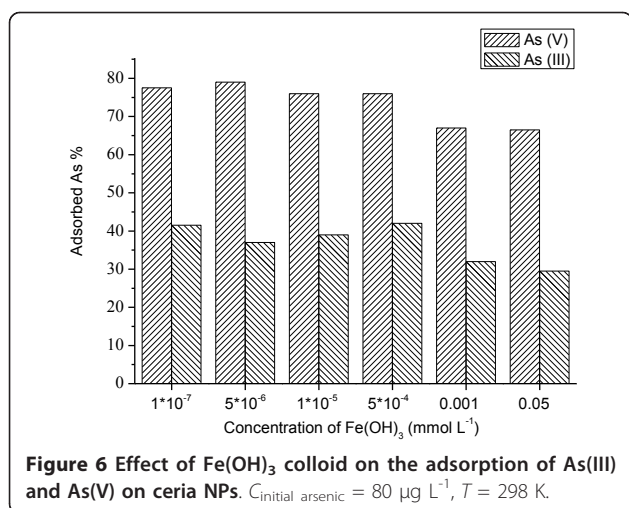


Figure 5 Effect of H₂SiO₃ colloid on the adsorption of As(III) and As(V) on ceria NPs. C_{initial arsenic} = 80 μg L⁻¹, T = 298 K.



of toxic chemicals, which may enhance the toxicity of toxic chemicals. It was found from Figure 6 that arsenic adsorption on ceria NPs increased stably with the increasing of H₂SiO₃ colloid concentration from 1 × 10⁻⁷ to 0.05 mmol L⁻¹; furthermore, ceria NPs had lower As(III) adsorption than As(V) adsorption under these conditions. Such a difference in As(III) and As(V) sorption efficiencies on ceria NPs could be related to possible differences between arsenic surface complexes on these different adsorbents. Interestingly, a recent study by Wang et al. [40] proposed that arsenate is absorbed more efficiently than arsenite on green rusts: for arsenate, the presence of binuclear bidentate double-corner complexes and mononuclear monodentate corner-sharing complexes at the surface of green rusts, and for arsenite, the presence of dimers of As(III) pyramids binding to the edges of the GR1Cl layers by corner sharing with FeO₆ octahedra. On the other hand, Raven et al. [39] observed that arsenite adsorption was higher than arsenate adsorption on ferrihydrite throughout the pH range of 3 to 11. These findings indicate that different ferrous-based compounds have different adsorption capacities for arsenic, which in turn complicates the adsorption behavior of arsenic in ceria NPs.

Conclusions

The high adsorption capacity and reversible adsorption of arsenic on ceria NPs clearly confirm that ceria NPs can interact with arsenic when they are released into the environment, which may influence the fate and behavior of arsenic and may enhance the toxicity of ENPs and/or arsenic. Taken together, the results indicate that studies dealing with the potential ecotoxicological effects of NPs for the environment have to be designed carefully in order to have the defined understanding between the NPs and the adsorbed chemicals in the environment.

Acknowledgements

This work is financially supported by the Ministry of Science and Technology of China (grant no. 2011CB933400), the Ministry of Environmental Protection of China (grant no. 201209012), the National Natural Science Foundation of China (grant nos. 10875136 and 10905062), and the China Postdoctoral Science Foundation (grant nos. 20090460520 and 201003155).

Authors' contributions

QF designed the study, performed the research, and prepared the manuscript. ZZ provided the experimental idea and advised the experimental design. YM synthesized the target material and performed the statistical analysis. XH participated in the adsorption experiments. YZ and ZC contributed to the experimental idea and drafted the manuscript. All authors read and approved the final manuscript.

Competing interests

The authors declare that they have no competing interests.

Received: 8 August 2011 Accepted: 23 January 2012

Published: 23 January 2012

References

- Stephen JK, Pedro JJ, Graeme EB, Teresa FF, Richard DH, Delina YL, Shaily M, Michael JM, Jamie RL: **Nanomaterials in the environment: behavior, fate, bioavailability, and effects.** *Environ Toxicol Chem* 2008, **27**:1825-2851.
- Grazyna B, Jerzy G, Pawel LU: **Nanoparticles: their potential toxicity, waste and environmental management.** *Waste Manage* 2009, **29**:2587-2595.
- Moore MN: **Do nanoparticles present ecotoxicological risks for the health of the aquatic environment?** *Environ Int* 2006, **32**:967-976.
- Fang J, Shan XQ, Wen B, Lin JM, Lu XC, Liu XD, Owens G: **Sorption and desorption of phenanthrene onto iron, copper, and silicon dioxide nanoparticles.** *Langmuir* 2008, **24**:10929-10935.
- Yan XM, Shi BY, Lu JJ, Feng CH, Wang DS, Tang HX: **Adsorption and desorption of atrazine on carbon nanotubes.** *J Colloid Interf Sci* 2008, **321**:30-38.
- Birbaum K, Brogioli R, Schellenberg M, Martinoia E, Stark WJ, Günther D, Limbach LK: **No evidence for cerium dioxide nanoparticle translocation in maize plants.** *Environ Sci Technol* 2010, **44**:8718-8723.
- Ludwig KL, Robert B, Elisabeth M, Rolf K, René G, Wendelin JS: **Removal of oxide nanoparticles in a model wastewater treatment plant: influence of agglomeration and surfactants on clearing efficiency.** *Environ Sci Technol* 2008, **42**:5828-5833.
- Chen JP, Patil S, Seal S, McGinnis JF: **Rare earth nanoparticles prevent retinal degeneration induced by intracellular peroxides, nature nanotechnology.** *Nature Nanotechnology* 2006, **1**:142-150.
- Zholobak NM, Ivanov VK, Shcherbakov AB, Shaporev AS, Polezhaeva OS, Baranchikov AY, Spivak NY, Tretyakov YD: **UV-shielding property, photocatalytic activity and photocytotoxicity of ceria colloid solutions.** *J Photoch Photobio B* 2010, **102**:32-38.
- Yuan Q, Duan HH, Li LL, Sun LD, Zhang YW, Yan CH: **Controlled synthesis and assembly of ceria-based nanomaterials.** *J Colloid Interf Sci* 2009, **335**:151-167.
- Thill A, Zeyons O, Spalla O, Chauvat F, Rose J, Auffan M, Flank AM: **Cytotoxicity of CeO₂ nanoparticles for *Escherichia coli*. Physico-chemical insight of the cytotoxicity mechanism.** *Environ Sci Technol* 2006, **40**:6151-6156.
- Safi M, Sarrouj H, Sandre O, Mignet N, Berret JF: **Interactions between sub-10-nm iron and cerium oxide nanoparticles and 3T3 fibroblasts: the role of the coating and aggregation state.** *Nanotechnology* 2010, **21**:145103.
- Hoecke KV, Quik JT, Mankiewicz-Boczek J, Schampelaere KA, Elsaesser A, Meeren PV, Barnes C, McKerr G, Howard VC, Meent DV, Rydzynski K, Dawson KA, Salvati A, Lesniak A, Lynch I, Silversmit G, Samber BD, Vincze L, Janssen CR: **Fate and effects of CeO₂ nanoparticles in aquatic ecotoxicity tests.** *Environ Sci Technol* 2009, **43**:4537-4546.
- Johnston BD, Scown TM, Moger J, Cumberland SA, Baalousha M, Linge K, Aerle R, Jarvis K, Lead JR, Tyler CR: **Bioavailability of nanoscale metal oxides TiO₂, CeO₂, and ZnO to fish.** *Environ Sci Technol* 2010, **44**:1144-1151.
- López-Moreno ML, Rosa G, Hernández-Viezas J, Castillo-Michel H, Botez CE, Peralta-Videa JR, Gardea-Torresdey JL: **Evidence of the differential biotransformation and genotoxicity of ZnO and CeO₂ nanoparticles on soybean (*Glycine max*) plants.** *Environ Sci Technol* 2010, **44**:7315-7320.

16. Lu K, Zhang ZY, He X, Ma YH, Zhou KB, Zhang HF, Bai W, Ding YY, Wu ZQ, Zhao YL, Chai ZF: Bioavailability and distribution of ceria nanoparticles in simulated aquatic ecosystems, quantification with a radiotracer technique. *J Nanosci Nanotechnol* 2010, **10**:8658-8662.
17. Niu JL, Asim A, Linda MR, Wang XH, Pappachan EK: Cardioprotective effects of cerium oxide nanoparticles in a transgenic murine model of cardiomyopathy. *Cardiovasc Res* 2007, **73**:549-559.
18. Huang JH, Ilgen G, Vogel D, Michalzik B, Hantsch S, Tennhardt L, Billitewski B: Emissions of inorganic and organic arsenic compounds via the leachate pathway from pretreated municipal waste materials: a landfill reactor study. *Environ Sci Technol* 2009, **43**:7092-7097.
19. Williams PN, Lei M, Sun GX, Huang Q, Lu Y, Deacon C, Meharg AA, Zhu YG: Occurrence and partitioning of cadmium, arsenic and lead in mine impacted paddy rice: Hunan, China. *Environ Sci Technol* 2009, **43**:637-642.
20. Arai Y, Lanzirotti A, Sutton S, Davis JA, Sparks DL: Arsenic speciation and reactivity in poultry litter. *Environ Sci Technol* 2003, **37**:4083-4090.
21. Chen CL, Li XL, Zhao DL, Tan XL, Wang XK: Adsorption kinetic, thermodynamic and desorption studies of Th(IV) on oxidized multi-wall carbon nanotubes. *Colloids Surface A* 2007, **302**:449-454.
22. Zhang F, Jin Q, Chan SW: Ceria nanoparticles: size, size distribution, and shape. *J Appl Phys* 2004, **95**:4319-4325.
23. Ma YH, Kuang LL, He X, Bai W, Ding YY, Zhang ZY, Zhao YL, Chai ZF: Effects of rare earth oxide nanoparticles on root elongation of plants. *Chemosphere* 2010, **78**:273-279.
24. Zhang J, Ju X, Wu ZY, Liu T, Hu TD, Xie YN: Structural characteristics of cerium oxide nanocrystals prepared by the microemulsion method. *Chem Mater* 2001, **13**:4192-4197.
25. Rane N, Zou H, Buelna G, Lin JYS: Sol-gel synthesis and properties of unsupported and supported mesoporous ceria membranes. *J Membrane Sci* 2005, **256**:89-97.
26. Shirvani M, Kalbasi M, Shariatmadari H, Nourbakhsh F, Najafi B: Sorption-desorption of cadmium in aqueous palygorskite, sepiolite, and calcite suspensions: isotherm hysteresis. *Chemosphere* 2006, **65**:2178-2184.
27. Sander M, Lu YF, Pignatello JJ: A thermodynamically based method to quantify true sorption hysteresis. *J Environ Qual* 2005, **34**:1063-1072.
28. Goldberg S: Competitive adsorption of arsenate and arsenite on oxides and clay minerals sabine goldberg. *Soil Sci Soc Am J* 2002, **66**:413-421.
29. Chakraborty S, Wolthers M, Chatterjee D, Charlet L: Adsorption of arsenite and arsenate onto muscovite and biotite mica. *J Colloid Interf Sci* 2007, **309**:392-401.
30. Buschmann J, Kappeler A, Lindauer U, Kistler D, Berg M, Sigg L: Arsenite and arsenate binding to dissolved humic acids: influence of pH, type of humic acid, and aluminum. *Environ Sci Technol* 2006, **40**:6015-6020.
31. Antelo J, Avena M, Fiol S, López R, Arce F: Effects of pH and ionic strength on the adsorption of phosphate and arsenate at the goethite-water interface. *J Colloid Interf Sci* 2005, **285**:476-486.
32. Vithanage M, Chandrajith R, Bandara A, Weerasooriya R: Mechanistic modeling of arsenic retention on natural red earth in simulated environmental systems. *J Colloid Interf Sci* 2006, **294**:265-272.
33. Arai Y, Elzinga EJ, Sparks DL: X-ray absorption spectroscopic investigation of arsenite and arsenate adsorption at the aluminum oxide-water interface. *J Colloid Interf Sci* 2001, **235**:80-88.
34. Catalano JG, Zhang Z, Fenter P, Bedzyk MJ: Inner-sphere adsorption geometry of Se(IV) at the hematite (100)-water interface. *J Colloid Interf Sci* 2006, **297**:665-671.
35. Su TZ, Guan XH, Gu GW, Wang JM: Adsorption characteristics of As(V), Se (IV), and V(V) onto activated alumina: effects of pH, surface loading, and ionic strength. *J Colloid Interf Sci* 2008, **326**:347-353.
36. Chen CL, Wang XK: Sorption of Th (IV) to silica as a function of pH, humic/fulvic acid, ionic strength, electrolyte type. *Appl Radiat Isotopes* 2007, **65**:155-163.
37. Xu RK, Wang Y, Tiwari D, Wang HY: Effect of ionic strength on adsorption of As(III) and As(V) on variable charge soils. *J Environ Sci* 2009, **21**:927-932.
38. Altundogan HS, Altundogan S, Tümen F, Bildik M: Arsenic adsorption from aqueous solutions by activated red mud. *Waste Manage* 2002, **22**:357-363.
39. Raven K, Jain A, Loeppert R: Arsenite and arsenate adsorption on ferrihydrite: kinetics, equilibrium, and adsorption envelopes. *Environ Sci Technol* 1998, **32**:344-349.
40. Wang YH, Morin G, Ona-Nguema G, Juillot F, Guyot F, Calas G, Brown GE: Evidence for different surface speciation of arsenite and arsenate on green rust: an EXAFS and XANES Study. *Environ Sci Technol* 2010, **44**:109-115.

doi:10.1186/1556-276X-7-84

Cite this article as: Feng et al.: Adsorption and desorption characteristics of arsenic onto ceria nanoparticles. *Nanoscale Research Letters* 2012 **7**:84.

Submit your manuscript to a SpringerOpen® journal and benefit from:

- Convenient online submission
- Rigorous peer review
- Immediate publication on acceptance
- Open access: articles freely available online
- High visibility within the field
- Retaining the copyright to your article

Submit your next manuscript at ► springeropen.com